

Article

## Preparation of TiO<sub>2</sub> Nanocrystallite Powders Coated with 9 mol% ZnO for Cosmetic Applications in Sunscreens

Horng-Huey Ko <sup>1</sup>, Hui-Ting Chen <sup>1</sup>, Feng-Ling Yen <sup>1</sup>, Wan-Chen Lu <sup>1</sup>, Chih-Wei Kuo <sup>2</sup>  
and Moo-Chin Wang <sup>1,\*</sup>

<sup>1</sup> Department of Fragrance and Cosmetic Science, Kaohsiung Medical University, 100 Shih-Chuan 1st Road, Kaohsiung 80708, Taiwan; E-Mails: hhko@kmu.edu.tw (H.-H.K.); htchen@kmu.edu.tw (H.-T.C.); flyen@kmu.edu.tw (F.-L.Y.); wclu@kmu.edu.tw (W.-C.L.)

<sup>2</sup> Department of Resources Engineering, National Chen Kung University, 1 Ta-Hsueh Road, Tainan 70101, Taiwan; E-Mail: jeffreykuo@passivecomponent.com

\* Author to whom correspondence should be addressed; E-Mail: mcwang@kmu.edu.tw; Tel.: +886-7-3121101 (ext. 2366); Fax: +886-7-3210683.

Received: 5 January 2012; in revised form: 18 January 2012 / Accepted: 18 January 2012 / Published: 3 February 2012

---

**Abstract:** The preparation of TiO<sub>2</sub> nanocrystallite powders coated with and without 9 mol% ZnO has been studied for cosmetic applications in sunscreens by a co-precipitation process using TiCl<sub>4</sub> and Zn(NO<sub>3</sub>)<sub>2</sub>·6H<sub>2</sub>O as starting materials. XRD results show that the phases of anatase TiO<sub>2</sub> and rutile TiO<sub>2</sub> coexist for precursor powders without added ZnO (T-0Z) and calcined at 523 to 973 K for 2 h. When the T-0Z precursor powders are calcined at 1273 K for 2 h, only the rutile TiO<sub>2</sub> appears. In addition, when the TiO<sub>2</sub> precursor powders contain 9 mol% ZnO (T-9Z) are calcined at 873 to 973 K for 2 h, the crystallized samples are composed of the major phase of rutile TiO<sub>2</sub> and the minor phases of anatase TiO<sub>2</sub> and Zn<sub>2</sub>Ti<sub>3</sub>O<sub>8</sub>. The analyses of UV/VIS/NIR spectra reveal that the absorption of the T-9Z precursor powders after being calcined has a red-shift effect in the UV range with increasing calcination temperature. Therefore, the TiO<sub>2</sub> nanocrystallite powders coated with 9 mol% ZnO can be used as the attenuate agent in the UV-A region for cosmetic applications in sunscreens.

**Keywords:** anatase; rutile; surface modification with 9 mol% TiO<sub>2</sub>; sunscreens cosmetic application; co-precipitation process

---

## 1. Introduction

Fine particles of various metal oxides, such as titanium oxide ( $\text{TiO}_2$ ) and zinc oxide ( $\text{ZnO}$ ) are extensively used as agents to attenuate (absorb and/or scatter) ultraviolet (UV) radiation, and have many describable characteristics, such as a long history of topical use, broad spectrum absorption, high photostability and low irritancy [1]. Nohynek *et al.* [2] have reported that modern sunscreens contain insoluble  $\text{TiO}_2$  or  $\text{ZnO}$  nanoparticles due to those are colorless and reflect/scatter UV light more efficiently than larger particles. The crystal structure of  $\text{TiO}_2$  has three different polymorphic forms: brookite (orthorhombic), anatase (tetragonal) and rutile (tetragonal). The UV-attenuating effect of  $\text{TiO}_2$  is dependent on the crystal structure, surface area, size distribution, porosity, surface hydroxyl density, *etc.*, as reported by Lee *et al.* [3]. However,  $\text{TiO}_2$  powders attenuate UV radiation more effectively only in the UVB region.

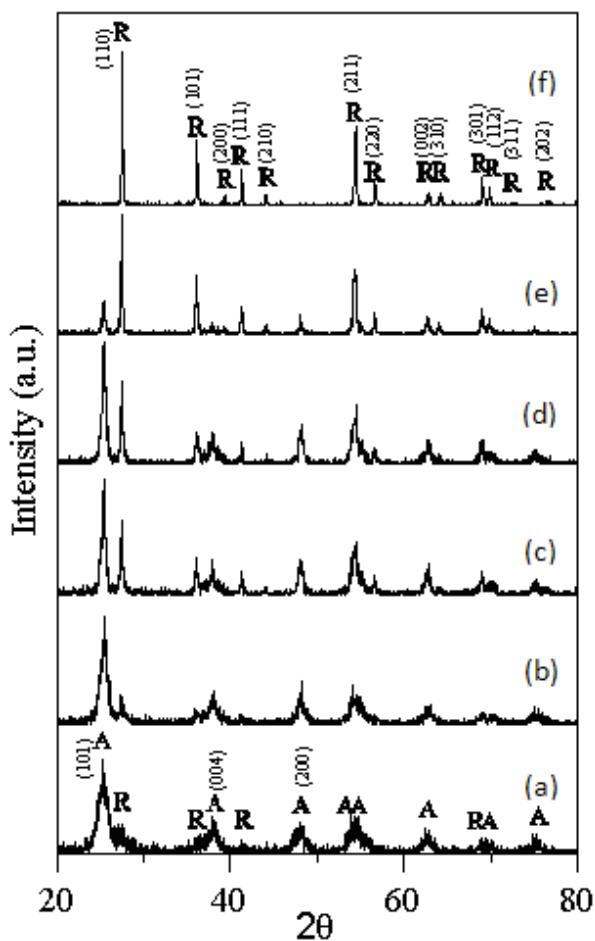
To increase the transparency and attenuate the UV radiation more effectively with a lower content of metal oxide particles, nano-sized primary single particles must be dispersed homogeneously into the medium [4]. In addition, the surface passivation of metal oxide nanoparticles with a layer of inorganic, organic, or bioactive materials to form the core-shell nanoparticles has attracted considerable attention [5]. A surface coating can be added to nanosized  $\text{TiO}_2$  to enhance its UV absorption by the diffraction mechanism of different light. The  $\text{TiO}_2$  surface coating with silica enhances UV-B absorption, but not UV-A absorption, as reported by Jaroenworarluck *et al.* [6]. Liao *et al.* [7] pointed out that the absorbance of amorphous  $\text{TiO}_2$ -coated  $\text{ZnO}$  nanoparticles at 375 nm gradually decreased with an increase in the molar ratio of Ti/Zn and time for the  $\text{TiO}_2$  coating, and that the emission intensity of  $\text{ZnO}$  cores could be significantly enhanced by the amorphous  $\text{TiO}_2$  shell. However, the studies of the  $\text{TiO}_2$  nanocrystallite powders coated with  $\text{ZnO}$  for sunscreens cosmetic applications have not been discussed in detail.

In order to promote the absorption of  $\text{TiO}_2$  nanocrystallite powders to UV-A region, the surface of  $\text{TiO}_2$  nanocrystallite powders must be modified. In the present work, an effort on the surface modification of  $\text{TiO}_2$  nanocrystallite powders coated with 9 mol%  $\text{ZnO}$  for cosmetic applications in sunscreens was studied using X-ray diffraction (XRD), transmission electron microscopy (TEM), selected area electron diffraction (SAED), and UV-vis absorption spectra. The aims of this paper are: (i) to study the phase transformation of  $\text{TiO}_2$  precursor powders with and without 9 mol%  $\text{ZnO}$ ; (ii) to observe the microstructure of  $\text{TiO}_2$  nanocrystallite powders with 9 mol%  $\text{ZnO}$ ; and (iii) to evaluate the UV absorption at 200–700 nm.

## 2. Results and Discussion

Figure 1 shows the XRD patterns of the T-0Z freeze dried precursor powders are calcined at various temperatures for 2 h. Figure 1a shows the T-0Z precursor powders are calcined at 523K for 2 h, and reveals that the crystalline phases of the powders were composed of the anatase and rutile  $\text{TiO}_2$ , but the crystallinity of rutile  $\text{TiO}_2$  was very poor. The crystallinity of rutile increased while the anatase decreased as the calcination temperature rose from 673 to 973 K (Figure 1b–d). When calcined at 1273 K for 2 h, XRD result (Figure 1f) shows that only rutile  $\text{TiO}_2$  appeared.

**Figure 1.** X-ray diffraction (XRD) patterns of the T-0Z freeze dried precursor powders are calcined at various temperatures for 2 h: (a) 523 K; (b) 673 K; (c) 773 K; (d) 873 K; (e) 973 K and (f) 1273 K (A: anatase, R: rutile).

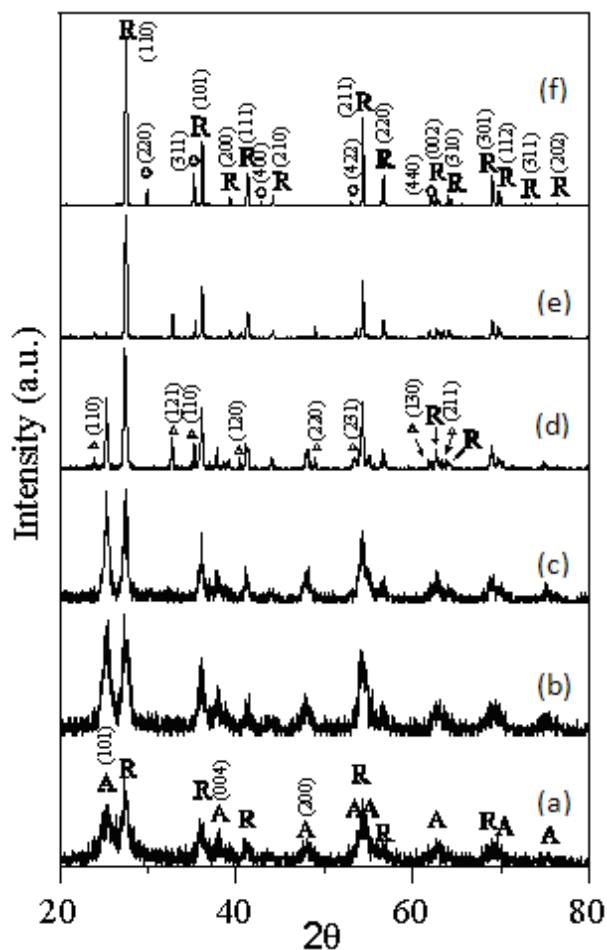


In the present study, the rutile  $\text{TiO}_2$  in T-0Z freeze dried precursor powders began to form at 523 K, and was the dominant phase when calcined at 973 K, and saw further increases as the calcination temperature rose. The anatase to rutile  $\text{TiO}_2$  transformation is affected by crystallite size, dopant type and concentration, as well as the titanium oxide precursor in solution chemical synthesis, as reported by Zhang and Banifield [8]. In fact, the phase transformation of anatase to rutile  $\text{TiO}_2$  is nucleated at anatase {112} twin boundaries, and the rutile nucleation involves the displacement of only half the titanium cations in the twin slab [9]. When the transformation is occurs continuously, slabs of anatase octahedral are destabilized, which results in a rapid progression of anatase into rutile  $\text{TiO}_2$ .

Figure 2 shows the XRD patterns of the T-9Z freeze dried precursor powders are calcined at various temperatures for 2 h. Figure 2a shows the XRD pattern of the T-9Z freeze dried precursor powders are calcined at 523 K for 2 h, and reveals that the crystallites are the coexisting phases of anatase and rutile  $\text{TiO}_2$ . It can also be seen in Figure 2b–f that the crystallinity of the rutile phase improved with the calcination temperature increase. However, the crystallinity of the anatase phase decreased with the rising calcination temperature. When calcined at 1273 K for 2 h (Figure 2f), the anatase  $\text{TiO}_2$  phase disappeared, but the rutile  $\text{TiO}_2$  still appeared. In addition, when the T-9Z freeze dried precursor powders are calcined at 873 K for 2 h, the minor phase of  $\text{Zn}_2\text{Ti}_3\text{O}_8$  first appeared (Figure 2d).

Moreover, the  $Zn_2Ti_3O_8$  transformed to  $Zn_2TiO_4$  when the T-9Z freeze dried precursor powders are calcined at 1273 K for 2 h (Figure 2f).

**Figure 2.** XRD patterns of the T-9Z freeze dried precursor powders are calcined at various temperatures for 2 h: (a) 523 K; (b) 673 K; (c) 773 K; (d) 873 K; (e) 973 K and (f) 1273 K (A: anatase; R: rutile;  $\Delta$ :  $Zn_2Ti_3O_8$ ;  $\circ$ :  $Zn_2TiO_4$ ).



In addition, although zinc oxide is not identified in the XRD patterns for the present study, Figure 2e indicates that the phases of  $Zn_2Ti_3O_8$  and  $Zn_2TiO_4$  were formed when T-9Z freeze dried precursor powders were calcined between 773 K and 1273 K for 2 h, respectively. The ionic radius of  $Ti^{4+}$  and  $Zn^{2+}$  are 0.68 Å and 0.74 Å, respectively. Since these values are almost equal, it can be inferred that the zinc ions did not insert into the structure of titanium, and instead were located at interstices or absorbed on the surface of  $TiO_2$ , thus forming the zinc-titanium solid solution [10].

The average crystallite size of the T-0Z and T-9Z freeze dried precursor powders calcination at various temperatures for 2 h is determined by Scherrer's formula [11]:

$$D = \frac{0.9\lambda}{\beta \cos\theta} \quad (1)$$

where  $D$  is the average crystallite size of the anatase and rutile  $TiO_2$ ,  $\lambda = 0.154$  nm is the X-ray wavelength of  $CuK\alpha$ ,  $\beta$  is the full width of the peak measured at half maximum intensity and  $\theta$  is the Bragg's angle of the peak.

The average crystallite size of the anatase and rutile phases  $\text{TiO}_2$  after it has been calcined at various temperatures for 2 h is obtained and listed in Table 1. It can be seen that the average crystallites of anatase and rutile  $\text{TiO}_2$  increase with calcination temperature increased but all sizes are smaller than 100 nm. These results reveal all crystallite sizes of anatase and rutile  $\text{TiO}_2$  in the nano-scale. Moreover, the crystallite size of rutile  $\text{TiO}_2$  in T-0Z is smaller than that in T-9Z when the freeze dried precursor powders are calcined at 1273 K for 2 h.

**Table 1.** The average crystallite size of anatase and rutile  $\text{TiO}_2$  when T-0Z and T-9Z freeze dried precursor powders are calcined at various temperatures for 2 h.

Calcination Temperature (K)	Crystallite Size T-0Z (nm)		Crystallite Size T-9Z (nm)	
	Anatase	Rutile	Anatase	Rutile
523	$6.5 \pm 0.2$	–	$5.0 \pm 0.2$	$5.7 \pm 0.2$
673	$9.8 \pm 0.3$	$13.2 \pm 0.2$	$8.6 \pm 0.2$	$10.0 \pm 0.2$
773	$15.5 \pm 0.3$	$21.0 \pm 0.4$	$12.9 \pm 0.2$	$15.7 \pm 0.2$
873	$16.5 \pm 0.3$	$28.9 \pm 0.4$	$31.4 \pm 0.4$	$34.0 \pm 0.4$
973	$20.4 \pm 0.4$	$37.4 \pm 0.5$	–	$48.6 \pm 0.4$
1273	–	$57.7 \pm 0.6$	–	$78.8 \pm 0.6$

“–” denotes the phase disappeared.

It is well known that the polymorphic transformation of ceramic materials generally depends on the nature of the dopant, amount of the dopant and the processing route. The additions of  $\text{Cr}_2\text{O}_3$  [12],  $\text{SiO}_2$  [13], and  $\text{CeO}_2$  [14,15] have been found to retard the anatase to rutile  $\text{TiO}_2$  transformation. Furthermore, the additions of  $\text{Fe}_2\text{O}_3$  [16] and  $\text{AlCl}_3$  [17] have been shown to enhance the anatase to rutile  $\text{TiO}_2$  transformation. In the present study, for the samples of T-0Z and T-9Z, the diffraction peaks show the anatase and rutile phases of  $\text{TiO}_2$  were simultaneously present from 523 to 973 K, but when calcined at 973 K for 2 h, the (110) intensity of rutile  $\text{TiO}_2$  was greater than the (101) intensity of anatase  $\text{TiO}_2$  for the T-0Z sample. In addition, when the T-9Z sample are calcined of 973 K for 2 h, the (101) intensity of anatase  $\text{TiO}_2$  was only residual, and thus insignificant. Comparing Figures 1a and 2a, it can be observed that the (110) intensity of anatase is greater than the (110) intensity of rutile  $\text{TiO}_2$  in Figure 1a, but the results are different in Figure 2a. These results prove that doping ZnO into  $\text{TiO}_2$  can enhance the anatase to rutile  $\text{TiO}_2$  transformation and shift the transformation to a lower temperature. This phenomenon occurs because the zinc oxide leading to the surface nucleation occurred on this polymorph [18].

The influence of the dopant ZnO on the structure of the T-9Z samples can be explained based on the changes caused by the dopant on the  $\text{TiO}_2$  surface [14]. Because the ionic radius of  $\text{Zn}^{2+}$  (0.74 Å) is greater than that of  $\text{Ti}^{4+}$  (0.68 Å), but smaller than that of oxygen (1.32 Å), the zinc ions were not introduced into the structure of titanium oxide matrix [10]. Therefore, the same deformation of the lattice structure and deformation energy produced by the zinc ions did not occur, and the zinc ions absorbed on the surface of titanium oxide created the nucleation sites and enhanced an unstable anatase phase transition to rutile. The anatase to rutile  $\text{TiO}_2$  transformation was nearly complete at 973 K, as the surface nucleation is favored for the dopant.

Moreover, although the concentration was only 9.0 mol% ZnO, the segregation of dopant on the surface of titanium oxide matrix promoted the  $\text{Zn}_2\text{Ti}_3\text{O}_8$  formation at 873 K in the ZnO- $\text{TiO}_2$  system.

Chang *et al.* [19] synthesized zinc titanate nanocrystal powder using a sol-gel process, and noted that the phase of the low temperature form of  $\text{ZnTiO}_3$  (*i.e.*,  $\text{Zn}_2\text{Ti}_3\text{O}_8$ ) first formed at 773 K, but had poor crystallinity. At 873 K, the crystalline phase of  $\text{ZnTiO}_3$  was identified, but traces of  $\text{Zn}_2\text{TiO}_4$  and rutile also appeared. Wang *et al.* [20] using hydrothermal process prepared the  $\text{Zn}_2\text{Ti}_3\text{O}_8$  powders for cosmetic applications have reported that the zinc titanium powders was obtained from the  $\text{TiCl}_4$ ,  $\text{Zn}(\text{NO}_3)_2 \cdot 6\text{H}_2\text{O}$  and  $\text{NH}_4\text{OH}$  solutions put in a thermostatic autoclave at 423 K for 1 h. When the zinc titanate powders are calcined at 873 K for 1 h, the  $\text{Zn}_2\text{Ti}_3\text{O}_8$ ,  $\text{ZnO}$  and anatase  $\text{TiO}_2$  coexisted. Dulin and Rase [10] have pointed out that when the  $\text{ZnO}$  content is less than 50 mol% and the temperature below 1218 K, only the phases of  $\text{Zn}_2\text{Ti}_3\text{O}_8$  and rutile  $\text{TiO}_2$  are present. In addition, the  $\text{Zn}_2\text{TiO}_4$  and rutile  $\text{TiO}_2$  appeared when the temperature was between 1218 and 1691 K. The results of the present study are in agreement with those of Dulin and Rase [10], and Chang *et al.* [19].

Figure 3 shows the bright field (BF) and dark field (DF) images, and selected area electron diffraction (SAED) pattern of T-0Z freeze dried precursor powders are calcined at 1273 K for 2 h. Figure 3a shows the BF image of the irregular crystallites morphology with a size of about 60 nm. In addition, Figure 3b shows the DF image of the Figure 3a. Figure 3c reveals the SAED pattern corresponding to the rutile  $\text{TiO}_2$  with zone axes (ZA) of  $[1\bar{1}0]$ . The SAED pattern also provides the evidence of the presence of the rutile  $\text{TiO}_2$  in T-0Z powders when calcined at 1273 K for 2 h. Moreover, the crystallite sizes in Figure 3a also correspond to the results of Table 1.

When the T-9Z freeze dried precursor powders are calcined at 1273 K for 2 h, the TEM microstructure and SAED pattern are shown in Figure 4. Figure 4a,b shows the BF and DF images, respectively. The crystallite sizes are observed to be about 80 nm. Figure 4c shows the SAED pattern of Figure 4b. The SAED pattern corresponds to the rutile  $\text{TiO}_2$  with  $\text{ZA} = [001]$ .

**Figure 3.** Transmission electron microscopy (TEM) microstructure and selected area electron diffraction (SAED) pattern of the T-0Z freeze precursor powders are calcined at 1273 K for 2 h: (a) bright field (BF) image; (b) dark field (DF) image and (c) SAED pattern. The SAED pattern corresponding to the rutile  $\text{TiO}_2$  with  $\text{ZA} = [1\bar{1}0]$ .

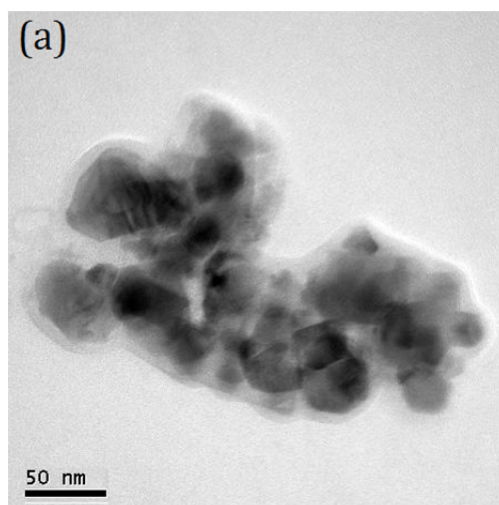


Figure 3. Cont.

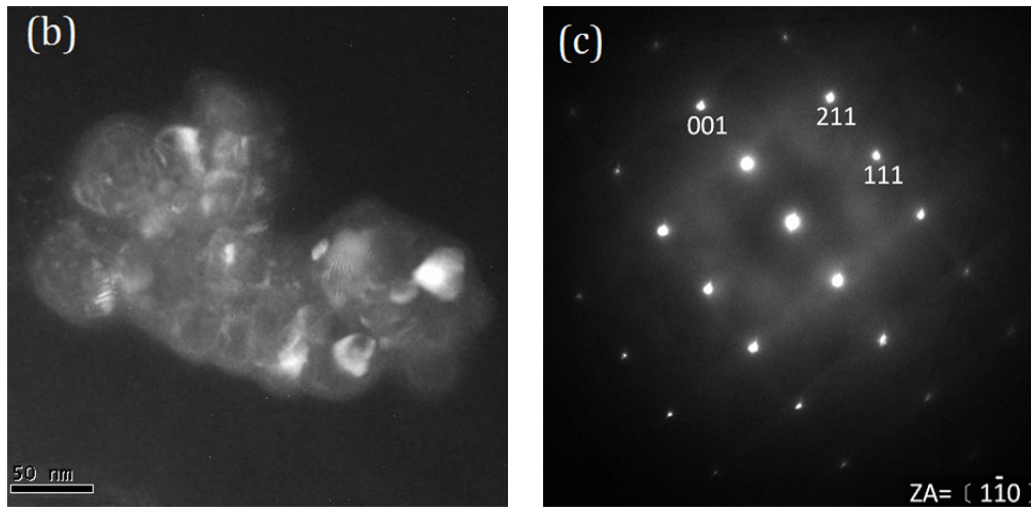
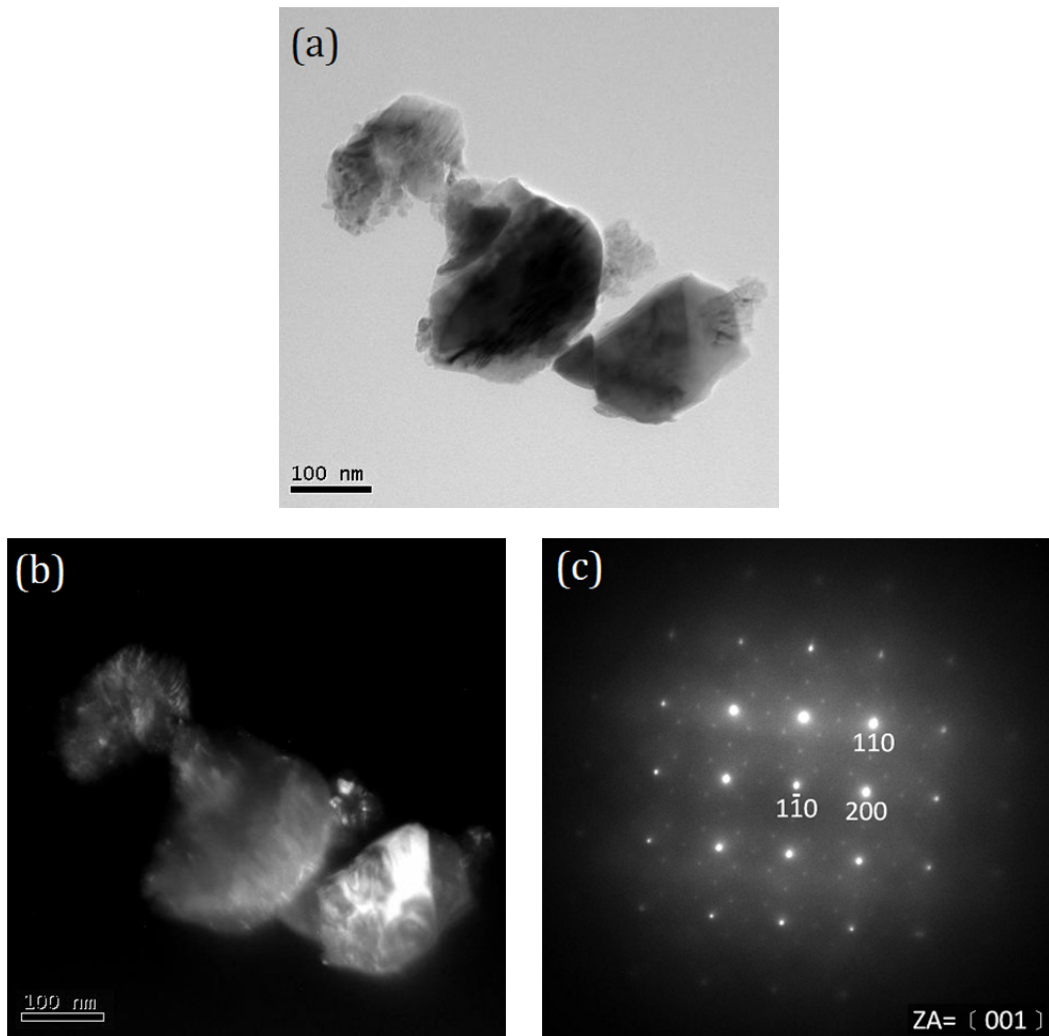


Figure 4. TEM microstructure and SAED pattern of the T-9Z freeze dried precursor powders calcined at 1273 K for 2 h: (a) BF image; (b) DF image and (c) SAED pattern. The SAED pattern corresponding to the rutile  $\text{TiO}_2$  with  $\text{ZA} = [001]$ .



**Figure 5.** TEM microstructure and SAED pattern of the T-9Z freeze dried precursor powders are calcined at 1273 K for 2 h: (a) BF image; (b) DF image; and (c) SAED pattern of fringe on (b). The SAED pattern corresponding to the  $\text{Zn}_2\text{TiO}_4$ .

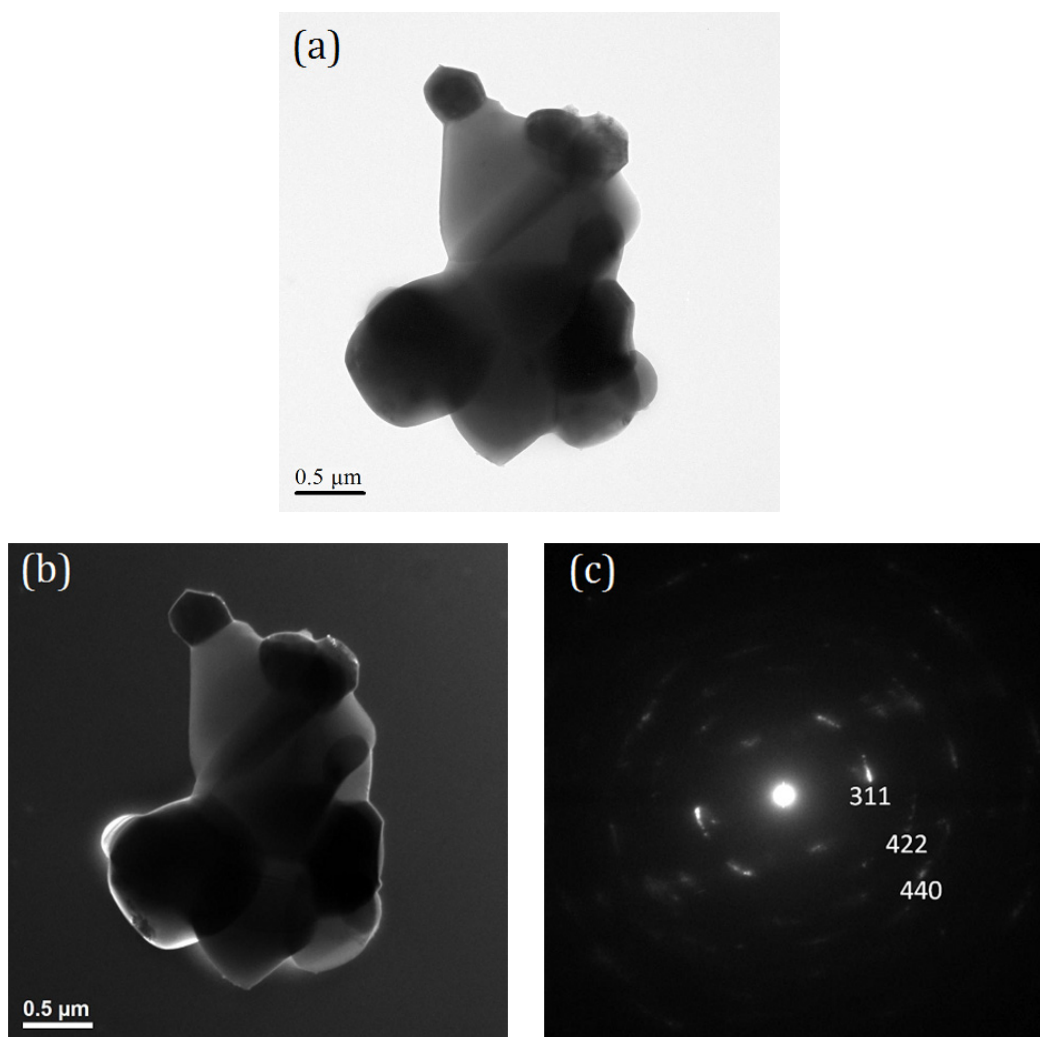
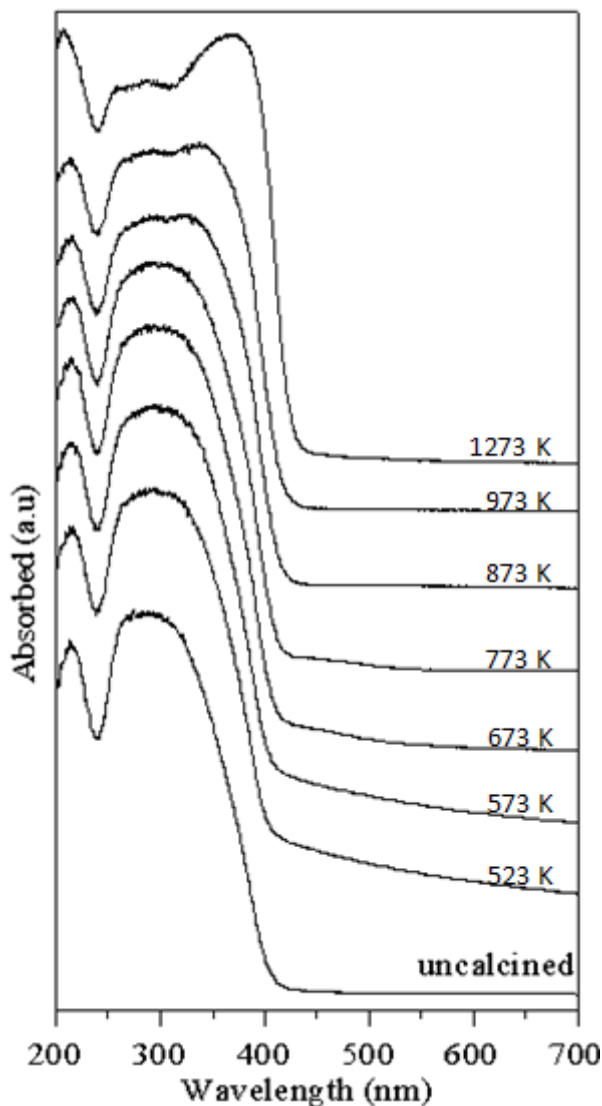


Figure 5a shows the BF image of the aggregate rutile crystallites in the irregular larger particle. Furthermore, the Figure 5b shows the fringe of the aggregate rutile  $\text{TiO}_2$ . Figure 5c shows the SAED pattern of the fringe in Figure 5b. The SAED pattern corresponds to the  $\text{Zn}_2\text{TiO}_4$ . The results from Figures 4c and 5c correspond to those of Figure 2f.

The relation of absorption and wavelength range between 200 and 700 nm for T-9Z freeze dried precursor powders calcined at various temperatures for 2 h are shown in Figure 6. It is found that the absorption of T-9Z powders in the UV range had a red-shift effect as the calcination temperature increased. This is because the quantity of photons reaching the core of a particle depends of the size and the optical properties of the  $\text{TiO}_2$  crystals. Maris *et al.* [21] also found that the penetration of light into a particle is influenced by the superficial morphology of the particles. Particles formed from larger  $\text{TiO}_2$  crystals have a smoother surface than those made from small crystals. On a smooth surface, the incident photons are scattered and mostly lost by reflection. In contrast, a rough surface allows a greater number of scattered photons to penetrate into the particle [15]. Moreover, the red-shift effect of

the TiO<sub>2</sub> nanocrystallite powders with surface modified by 9 mol% ZnO and calcined at 1273 K for 2 h indicates that they can be used as an UV-A attenuating agents for cosmetic applications in sunscreens.

**Figure 6.** Relation of the absorbed and wavelength range between 200 and 700 nm of the T-9Z freeze dried precursor powders calcined at various temperatures for 2 h.



Most of the UV absorbers used in sunscreens are oil-soluble or even oil-miscible and consequently are incorporated into the oil phase of sunscreen emulsions [22]. Moreover, Herzog *et al.* [22] also pointed out that the UV-attenuating efficiency increased with decreasing particle size up to a maximum particle size of 80 nm. With smaller particles, the extinction started to decrease again. Moreover, for the inorganic TiO<sub>2</sub> used as absorber at a particle size of 100 nm, the scattering that contributes to about 50% to the overall extinction in the range of the extinction maximum of the spectrum has been reported by Robb *et al.* [23]. On the other hand, Popov *et al.* [24] pointed out that the TiO<sub>2</sub> fine particles are embedded with sunscreens into the skin to effectively attenuate UV-B radiation. Moreover, TiO<sub>2</sub> particles with a size of 62 nm are found to be the most effective in protecting skin against UV-B radiation. As mentioned above, the results of the present study show a red-shift effect in the UV range.

Therefore, the TiO<sub>2</sub> nanocrystallite powders with surface modified by 9 mol% ZnO and calcined at 1273 K for 2 h can be used as an UV-A light attenuating agent for cosmetic applications in sunscreens.

### 3. Experimental Procedure

#### 3.1. Sample Preparation

The starting materials were reagent-grade TiCl<sub>4</sub> solution (purity ≥ 98.0%, supplied by Fluka, France), Zn(NO<sub>3</sub>)<sub>2</sub>·6H<sub>2</sub>O (purity ≥ 98%, supplied by Alfa Aersor, USA), 25 vol% ammonia solution (NH<sub>4</sub>OH, supplied by Riedel-de Haën, Germany) and polyethylene glycol (PEG, supplied by Nippon Shiyaku Kogyo K.K., Japan). A TiCl<sub>4</sub> solution of 0.5 M was prepared from 1 mol TiCl<sub>4</sub> solution dissolved in 2 L deionized water. The TiCl<sub>4</sub> aqueous solution was then supplemented with 1 wt% of PEG as a dispersant. The mixed solution was stirred and heated to 333 K for 6 h (denoted as solution I). NH<sub>4</sub>OH was then added to solution I until pH = 9. The mixed solution was then stirred at room temperature for 24 h to obtain white precipitates (denoted as T-0Z).

An aqueous solution of 9 mol% ZnO was prepared from the Zn(NO<sub>3</sub>)<sub>2</sub>·6H<sub>2</sub>O dissolved in deionized water and stirred at 273 K for 2 h (denoted as solution II). Solution II was then added slowly at a rate of 0.05 cm<sup>3</sup>·min<sup>-1</sup> with vigorous agitation in solution I at room temperature. At the end of titration, a syringe was used to minimize the size of falling drops and reduce the local reaction effect. During the whole process, the pH value was kept at 9 by adjusting the amount of NH<sub>4</sub>OH. The mixed solution was then stirred at room temperature for 24 h to obtain white precipitates (denoted as T-9Z).

After precipitation, the precipitates were washed thoroughly two times with a large amount of ethanol (purity ≥ 99.85%, supplied by J.T.Baker, USA) to remove NH<sub>4</sub>NO<sub>3</sub> [25]. Subsequently, the precipitates were freeze dried at 218 K in a vacuum.

#### 3.2. Sample Characterization

The crystalline phase was identified using an X-ray diffractometer (XRD, model Rad IIA, Rigaku Co., Tokyo, Japan) with Cu K $\alpha$  radiation and a Ni filter, operated at 30 kV, 20 mA and a scanning rate ( $2\theta$ ) of 0.25°·min<sup>-1</sup>. The microstructure of the powders before and after calcination was observed by transmission electron microscopy (TEM, model HF-2000, Hitachi Ltd., Tokyo, Japan), operating at 200 kV. The selected area electron diffraction (SAED) examination was conducted on the calcined samples. The UV-shielding was measured with a UV-vis spectrometer (Optometrics, SPF-290, Ayer, MA, USA).

### 4. Conclusions

- (1) The rutile TiO<sub>2</sub> began to form at 523 K of T-0Z freeze dried precursor powders, and was the dominant phase when calcined at 973 K for 2 h.
- (2) The anatase and rutile TiO<sub>2</sub> phases coexist in T-9Z powders when the calcination temperature is below 973 K. When calcined at 1273 K for 2 h, the anatase phase disappears. In addition, the Zn<sub>2</sub>Ti<sub>3</sub>O<sub>8</sub> first forms when T-9Z freeze dried precursor powders are calcined at 973 K for 2 h. When the T-9Z precursor powders are calcined at 1273 K for 2 h, the Zn<sub>2</sub>TiO<sub>4</sub> forms and the Zn<sub>2</sub>Ti<sub>3</sub>O<sub>8</sub> disappears.

- (3) The average crystallite sizes of anatase and rutile TiO<sub>2</sub> increase with increasing the calcination temperature, but all average crystallite sizes of anatase and rutile TiO<sub>2</sub> are smaller than 100 nm for T-0Z and T-9Z freeze dried precursor powders as calcined between 523 and 1275 K for 2 h. In addition, the crystallite size of rutile TiO<sub>2</sub> in T-0Z is smaller than that in T-9Z when the freeze dried precursor powders are calcined at 1273 K for 2 h.
- (4) The absorption of T-9Z powders in the UV range has a red-shift effect as the calcination temperature increases. This result shows that TiO<sub>2</sub> nanocrystallite powders added with 9 mol% ZnO and calcined at 1273 K for 2 h can be used as an UV-A attenuating agent for cosmetic applications in sunscreens.

### Acknowledgments

This work was supported by the National Science Council, Taiwan, the Republic of China under Contract No. NSC 100-2221-E-037-001 and NSC 99-2313-B-037-001-MY3, which is gratefully acknowledged. The authors sincerely thank M.H. Hom for advices on the manuscript and preparation.

### References

1. Al-Hilli, S.M.; Willander, M. Optical properties of zinc oxide nano-particle embedded in dielectric medium for UV region: Numerical simulation. *J. Nanoparticle Res.* **2006**, *8*, 79–97.
2. Nohynek, G.J.; Lademann, J.; Ribaud, C.; Roberts, M.S. Grey goo on the skin? Nanotechnology, cosmetic and sunscreen safety. *Crit. Rev. Toxicol.* **2007**, *37*, 251–277.
3. Lee, W.; Shen, H.S.; Dwight, K.; Wold, A. Effect of silver on the photocatalytic activity of TiO<sub>2</sub>. *J. Solid State Chem.* **1998**, *106*, 288–294.
4. Fairhurst, D.; Mitchnick, M.A. *Sunscreen-Development, Evaluation and Regulatory Aspects*, 2nd ed.; Lowe, N.J., Shaath, N.A., Pathak, M.A., Eds.; Marcel Dekker: New York, NY, USA, 1997; pp. 3–33.
5. Zhong, C.J.; Maye, M.M. Core-shell assembled nanoparticles as catalysis. *Adv. Mater.* **2001**, *13*, 1507–1511.
6. Jaroenworoluck, A.; Sunsaneeyamethe, W.; Kosachan, N.; Stevens, R. Characteristics of silica-coated TiO<sub>2</sub> and its UV absorption for sunscreen cosmetic applications. *Surf. Interface Anal.* **2006**, *38*, 473–477.
7. Liao, M.H.; Hsu, C.H.; Chen, D.H. Preparation and properties of amorphous titania-coated zinc oxide nanoparticles. *J. Solid State Chem.* **2006**, *179*, 2020–2026.
8. Zhang, H.; Banfield, J.F. Phase transformation of nanocrystalline anatase-to-rutile via combined interface and surface nucleation. *J. Mater. Res.* **2000**, *15*, 437–448.
9. Li, G.; Li, L.; Boerio-Goates, J.; Woodfield, B.F. High purity anatase nanocrystals: Near room temperature synthesis, grain growth kinetics, and surface hydration chemistry. *J. Am. Chem. Soc.* **2005**, *127*, 8659–8666.
10. Dulin, P.H.; Rase, D.E. Phase equilibria in the system ZnO-TiO<sub>2</sub>. *J. Am. Ceram. Soc.* **1960**, *43*, 125–131.
11. Cullity, B.D. *Elements of X-ray Diffraction*, 2nd ed.; Addison-Wesley Publishing Company: Reading, MA, USA, 1978; p. 87.

12. Wilke, K.; Breuer, H.D. The influence of transition metal doping on the physical and photocatalytic properties of titania. *J. Photochem. Photobiol. A* **1999**, *121*, 49–53.
13. Zhou, Y.S.; Fan, X.H. Preparation and properties of the nanometer composite oxide TiO<sub>2</sub>-SiO<sub>2</sub>. *Chem. J. Chin. Univ.* **2003**, *7*, 1266–1270.
14. Jing, L.; Sun, X.; Cai, W.; Li, X.; Fu, H.; Hou, H.; Fan, N. Photoluminescence of Ce doped TiO<sub>2</sub> nanoparticles and their photocatalytic activity. *Acta Chim. Sin.* **2003**, *61*, 1241–1245.
15. Yan, Q.Z.; Su, X.T.; Huang, Z.Y.; Ge, C.C. Sol-gel auto-igniting synthesis and structural property of cerium-doped titanium dioxide nanosized powders. *J. Eur. Ceram. Soc.* **2006**, *2b*, 915–921.
16. Hirano, M.; Joji, T.; Inagaki, M. Direct formation of iron (III)-doped titanium oxide (anatase) by thermal hydrolysis and its structure property. *J. Am. Ceram. Soc.* **2004**, *87*, 35–41.
17. Gesenhues, U.; Rentschler, T. Crystal growth and defect structure of Al<sup>3+</sup>-doped rutile. *J. Solid. State Chem.* **1999**, *143*, 210–218.
18. Inagaki, M.; Nakazawa, Y.; Hirano, M.; Kobayashi, Y.; Toyoda, M. Preparation of stable anatase-type TiO<sub>2</sub> and its photocatalytic performance. *Int. J. Inorg. Mater.* **2001**, *3*, 809–811.
19. Chang, Y.S.; Chang, Y.H.; Chen, I.G.; Chen, G.J.; Chai, Y.L. Synthesis and characterization of zinc titanate nano-crystal powders by sol-gel technique. *J. Cryst. Growth* **2006**, *243*, 319–326.
20. Wang, C.L.; Hwang, W.S.; Chang, K.M.; Ko, H.K.; Hsi, C.S.; Huang, H.H.; Wang, M.C. Formation and morphology of Zn<sub>2</sub>Ti<sub>3</sub>O<sub>8</sub> powders using hydrothermal process without dispersant agent or mineralizer. *Int. J. Mol. Sci.* **2011**, *12*, 935–945.
21. Maria, A.J.; Yeung, K.L.; Lee, C.Y.; Yue, P.L.; Chan, C.K. Size effect in gas-phase photo-oxidation of trichloroethylene using nanometer-sized TiO<sub>2</sub> catalysts. *J. Catal.* **2000**, *192*, 185–196.
22. Herzog, B.; Quass, K.; Schmidt, E.; Mller, S.; Luther, H. Physical properties of organic particulate UV absorbers used in sunscreens II. UV-attenuating efficiency as function of particle size. *J. Colloid Interface Sci.* **2004**, *276*, 354–363.
23. Robb, J.L.; Simpson, L.H.; Tunstall, D.F. Scattering & absorption of UV radiation by sunscreens containing fine particle & pigmentary titanium dioxide. *Drug Cosmet. Ind.* **1994**, *154*, 32–39.
24. Popov, A.P.; Priezzhev, A.V.; Lademann, J.; Myllyla, R. TiO<sub>2</sub> nanoparticles as an effective UV-B radiation skin-protective compound in sunscreens. *J. Phys. D* **2005**, *38*, 2564–2570.
25. Kuo, C.L.; Wang, C.L.; Ko, H.H.; Hwang, W.S.; Chang, K.M.; Li, W.L.; Huang, H.H.; Chang, Y.H.; Wang, M.C. Synthesis of zinc oxide nanocrystalline powders for cosmetic applications. *Ceram. Int.* **2010**, *36*, 693–698.